Mapping of Tsunami Hazard along Makran Coast of Pakistan

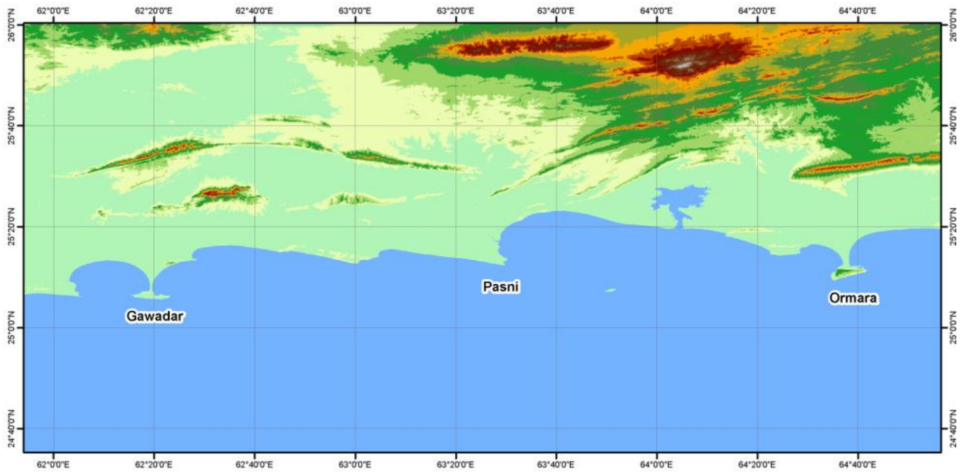

by

Nasir Mahmood, Karam Khan, Zahid Rafi and Dr. Finn Løvholt

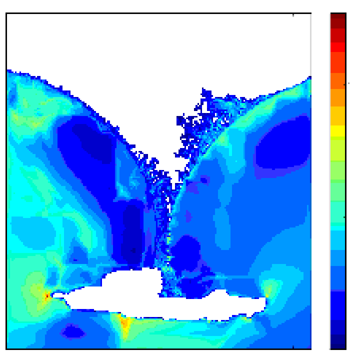

Norges Geotekniske Institutt

Technical Report No. PMD -20 /2012
February, 2012

Acknowledgement

This work was carried out at Norwegian Geotechnical Institute (NGI), Norway. We are grateful to Dr. Carl Bonnevie Harbitz for his valuable expertise and encouraging interest to our work and useful discussions. We acknowledge Dr. Gunilla Kaiser, Mr. Lasse Scheele and Dr. Sylfest Glimsdal for supporting us in GIS and GMT tools. This project is supported by Norwegian Ministry for Foreign Affairs. Thanks are expressed to Director General, Pakistan Meteorological Department for providing the opportunity to work in a leading international centre for research in geosciences.

Table of Contents

List of Figures

List of Tables

Preface

Tsunami is one of the most significant oceanic hazards generally triggered by earthquakes and submarine landslides. Tsunami might affect not only the area where it is generated but also damage localities which are located far away from the generation region. It is believed that technology alone cannot protect coast's habitats in case of near-source tsunami. Communities and local authorities need to be aware of which areas are likely to be flooded. Local decision-makers need to understand the risk. The following issues are considered for tsunami response plan;

i- Use of Inundation maps
ii- Development of tsunami evacuation plan

Pakistan Meteorological Department (PMD) has established a Tsunami Early Warning System with the financial as well as technical support of UNESCO-IOC. These systems are installed at Karachi and Islamabad. The only missing field was the tsunami modeling for Makran coast of Pakistan. Modeling, inundation and run up, is an essential components of tsunami studies at scientific and operational level. For the mapping of inundation and run up of water, selection of maximum credible earthquake, historical data, bathymetric, topographic data of high resolution and selection of possible tsunami scenarios are required. Tsunami modeling and risk analysis of coastal areas are needed for better preparedness and effective mitigation strategy during and after tsunami.

The model incorporated in this research report covered the generation, propagation, travel time, inundation and run up of tsunami. The coast line of Pakistan has experienced a disastrous tsunami on 1945 when an earthquake of magnitude 8.0 occurred in the Arabian Sea which generated tsunami. Although, the population density along the Makran coast was very low even then the casualties were more than 4000. Arabian Sea cannot be ignored due to its earthquake potential as Makran subduction zone is located about hundred kilometers away from the coast. Through this study, efforts have been made to identify the critical need to develop the inundation maps for the local communities at risk. It also helps the residents to understand the multi-hazard ramifications of major earthquake and its disruption to the community.

This study is carried out under "Institutional Cooperation Program Pak-3004" concerning earthquake risk of Pakistan & Tsunami modeling for Makran coast. This project is supported by Ministry of Foreign Affairs of Government of Norway through Ministry of Planning & Development Division. It is the first effort to prepare the tsunami model for three coastal cities like Gwadar, Pasni and Ormara.

M/S. Nasir Mahmood and Karam Khan with M/S Zahid Rafi and Dr. Finn Løvholt of NGI (Norwegian Geotechnical Institute) co-authored this research study. I am really pleased to see the amount of work and the way they have done at NGI and at PMD Islamabad.

(Arif Mahmood)
Director General

Abstract

The study on tsunami scenarios along the Makran coast of Pakistan was made due to available history of earthquakes in the region. Tsunami inundation maps have been produced to identify areas susceptible to tsunami hazard for the coastal cities of Gwadar, Pasni and Ormara. A range of earthquakes source scenarios including moment magnitudes of 7.7, 8.1, 8.5, and a mega thrust of 9.0 were modeled. The three lowest magnitudes are considered as possible, based on previous events, whereas the possibility of an Mw 9.0 event is more doubtful. However, assessment of the likelihood for the scenarios is left to a later study. The scenarios are constructed based on superposition of available sources in MOST (Method of Splitting Tsunami), which is the simulation tool, applied in the current study. We construct a hierarchy of three grids using best available topography, bathymetry data resources with GIS and Matlab tools. Simulations are carried out for tsunami arrival times, water levels, current velocities and inundation maps are prepared. The results of modeling show that all the three coastal points are inundated heavily in our worst case scenario with maximum water levels in the range of 1 – 7 m, with severe inundation occurring for the Mw 8.5 and 9.0 events only. The first tsunami wave strikes the coast within 12-20 minutes of earthquake occurrence being close to the source. The applied MOST sources are interpreted with a very shallow dip which most likely underestimate the height of the initial elevation, and as a consequence, the run-up. Additional simulations with increased dip angle should therefore be carried out in a later stage. The computational grids also need further amendment. The last two issues, in addition to assessing scenario probabilities, are crucial with respect to establishing proper tsunami hazard map for the exposed locations.

Key Words: *Tsunami inundation, Bathymetry, Numerical Simulations, Maximum water level*

1. Introduction

1.1 Background and Objectives

History of large earthquakes along the Makran Subduction Zone (MSZ) provides an evidence of the potential tsunami hazard for the entire coast of Pakistan. The fast growing cities of Gwadar, Pasni and Ormara are likely to be the most vulnerable to tsunami due to being much closed to the Subduction zone. Similarly the most populous city and the economic hub of Pakistan, i.e. Karachi may also experience inundation due to tsunami from MSZ. MSZ extends eastward from the strait of Hermuz in Iran to near Karachi (page et al. 1979).
The study presented in this paper was done at Norwegian Geotechnical Institute (NGI) with the aims to assist the local authorities in Pakistan by development of plans for how to deal with the future tsunami hazard and risk along Makran coast in a short term, as well as in a long term perspective. Inundation maps for three selected coastal points were prepared to identify areas susceptible to tsunami hazard. As a first step to develop a reliable early tsunami warning system, to indicate the evacuation roots and emergency shelter locations. The identification of possible tsunami source areas was based on the historic record of regional tsunamigenic earthquakes. The 1200 km long (MSZ) is seismically not as active as the Himalaya or Sunda Arc, but has produced great earthquakes and tsunamis in the past (Jaiswal et al. 2009). A field survey of the Iranian coastline and Makran coast suggested that the raised beaches and terraces confirm the tectonic model of a subduction zone off the coast of Pakistan and Iran (Page et al. 1979).
We estimate tsunami inundation maps for hazard assessment for the cities of Gawadar, Pasni and Ormara by modeling four scenario earthquakes including one mega-thrust earthquake Mw 9.0. Modern seismicity indicates that the plate boundary in western Makran is completely silent since from the last few decades, but a large event in 1483 may have ruptured western Makran (Byrne et al. 1992). The plate boundary therefore, in western Pakistan may experience larger magnitudes with longer recurrence period. The large changes in seismicity between eastern and western Makran suggest segmentation of the Subduction zone. The absence of plate boundary events in western Makran indicates that either there is aseismic Subduction or plate boundary is currently locked. The presence of well defined late Holocene terraces along the eastern and western Makran are capable of producing large plate boundary earthquakes (Byrne et al. 1992). We have modeled a mega thrust event in our study. The likelihood or possibility of such a large magnitude event is left for further study. Another possibility is that Makran has a large accetionary wedge and the possibility of a tsunami generation due to underwater landslide cannot be ruled out; the issue needs to be further investigated.

1.2 Geology and Tectonics of the Study Area

Makran is located at the coast of Northern Arabian Sea and is land of three important cities of Pakistan; Gwadar, Pasni and Ormara. The Zendan – Minab fault system and the accetionary front defines the western and southern boundary of the Makran accetionary complex respectively (Mokhtari et al. 2008) outlined in Figure 1.

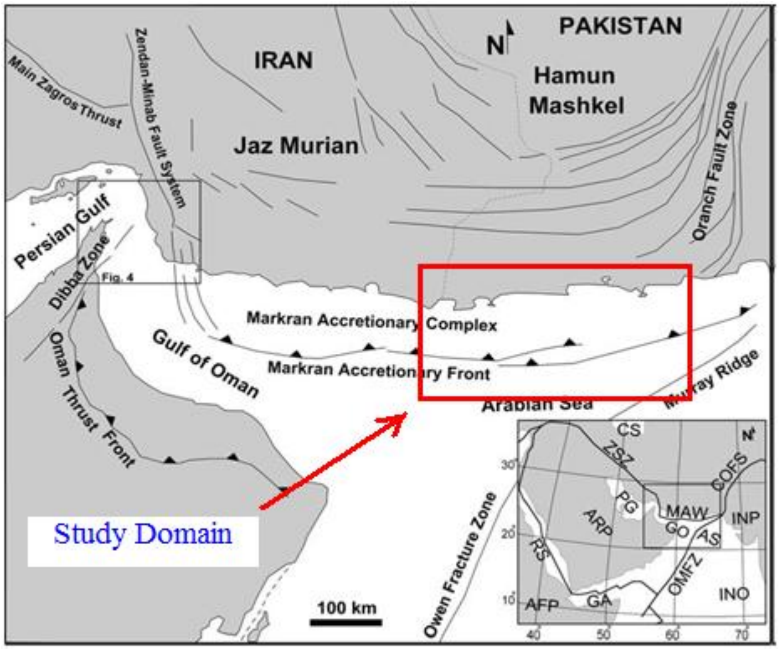

Figure 1 Study Domain and tectonic setting around Makran (Mokhtari et al.2008)

The Ornach-Nal fault zone is located in the eastern side of this complex and is said to be the western boundary of the Indian plate. Murray ridge system defines the offshore boundary of the Arabian and Indian plates. Further southward Owen Fracture Zone demarcates the boundary between Indian plate and Arabian plate.

Makran Subduction Zone runs east-west from Strait of Hormuz in Iran to the Ornach-Nal fault in Pakistan in the West of Karachi. Makran subduction occurred throughout the late Mesozoic and Cenozoic up till now; the Cenozoic rocks shape a vast accertionary prism (Musson R. M. W. British Geological Survey). Accertionary wedge is composed of distorted sediments ranging in age from late Cretaceous to-date (Harma et al 1982). Makran is a large sedimentary prism accerted during the Cenzoic (Farhoud et al 1977). S. Sirtajuddin A. 1969 has revealed Clastic sedimentation in southern Makran from Oligocene, forming a wedge thickening seaward to a total thickness of at least 10 km along the coast of Arabian Sea. The types of rocks found include shale, mudstone, conglomerate and minor coquina and limestone.

1.3 Historical events in Makran

Seven large earthquakes have been reported in the history of Makran. An earthquake in 1483 affected the state of Hormuz and Northern Oman and may have occurred somewhere in western Makran (Byrne et al. 1992). It is the only event reported in the history of Western Makran. Another event in 1765 was felt strongly in eastern most Makran. Two coastal events occurred in 1851 and 1864 affecting the town of Gwadar. Walton, Director of Makran Coast and Sub-Marine Telegraph Department wrote the following letter to the Secretary Government, Bombay, India, confirming the 1864 event another event which happened almost 100 years ago (1851) when he informed, that an entire hill, with men and camels on it, disappeared into the sea. He was of opinion that there must have been a landslip caused by some sub-marine disturbance. (Bombay

Geology Society No. 622 of 1864 p. cxxv) Another large event occurred in Northern Makran in 1914. In 1945 a great earthquake smashed the coast of eastern Makran near Pasni. This is the only event which is well documented. An aftershock followed this event in 1947 (Byrne et al. 1992.). The 1945 Makran earthquake (Mw 8.1-8.3) is considered to be the characteristic earthquake because it is most destructive and largest event in the region and enough information is available about the seismic factors (Heiderzaeh et al 2009). Numbers of authors have agreed a thrust faulting source mechanism for 1945 event because of its location at a subduction zone and its large magnitude. The 1945 earthquake caused extensive damage along the Makran coast and generated a large tsunami. A magnitude of Mw 8.3 is assigned to this event (Page et al. 1979). Epicenter of this event was located at 25.1°N and 63.48 °E and with a magnitude of Mw 8.1 and seismic moment Mo as 1.8×10^{21} N-m (Byrne et al. 1992). Occurrence of several waves separated by two hours as well as rupturing of the Mumbai-London telegraph cable suggested that the earthquake triggered a delayed underwater landslide (Ambraseys et al. 1982). The initial wave shortly after the event did not intrude significantly; destructive tsunami that swept Pasni occurred 2 – 2 ½ hours after the earthquake (Pendse, 1948). Tsunami heights at Pasni and Ormara were reported to be in the range of 5 – 10 m (Pendse, 1948). Local inhabitants report that three tsunamis hit the Makran coast 1 ½ - 2 hours after the earthquake reaching a height of 7 – 10 m (Page et al. 1979).Coastal uplift associated with 1945 earthquake was 2 meter (page et al. 1979). Slight damage at Gwadar and greater eastward and northeastward of Pasni and large uplift of Ormara suggested that most of the rupture area lies east of Pasni (Byrne et al. 1992). Byrne et al. 1992 assumed that similar events could return at least every 175 years in eastern Makran where as Page et al. 1979 estimate the recurrence of a similar type earthquake along Makran Subduction zone in approximately 125 – 250 years.

2. Methodology and Approaches

2.1 Scope of Study Area

The domain of study area ranges from 24ºN to 26ºN and 61ºE to 65ºE. Three coastal points Gawadar, Pasni and Ormara included in our study are shown in Figure 2. The area as been prone to great earthquakes and tsunamis in the past.

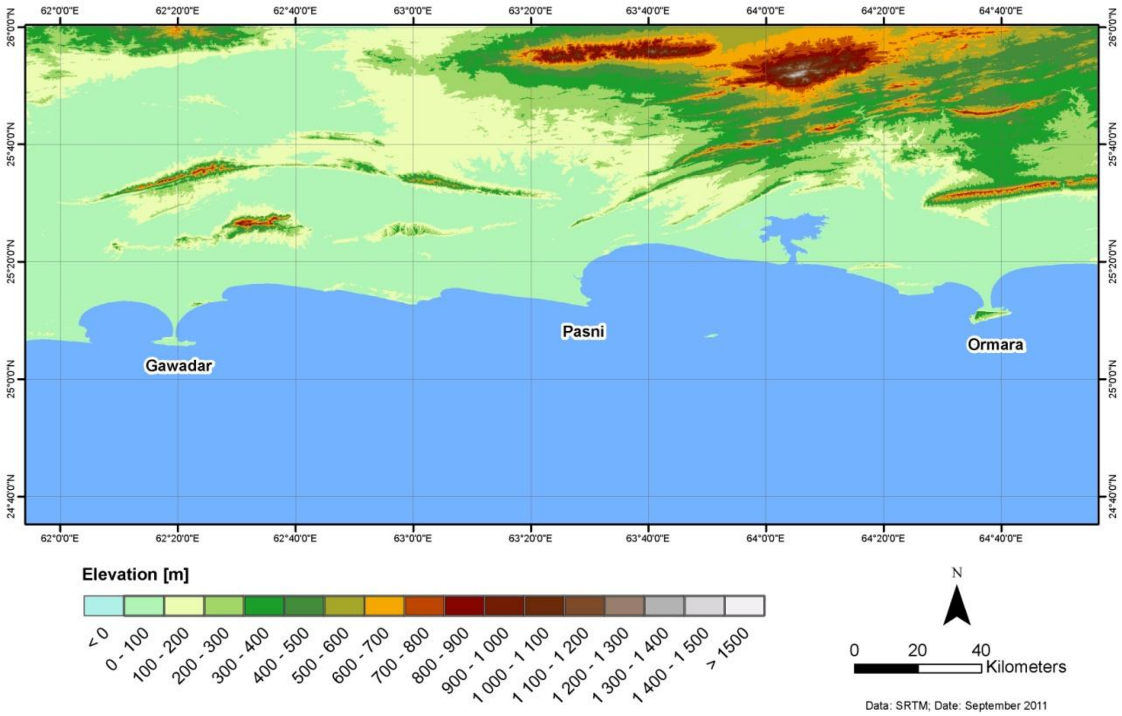

Figure 2 Overview of Makran Coast and study domain showing land elevation

2.2 Bathymetry and Topography Data

We construct a hierarchy of three grids A, B and C using best available topography and bathymetry data resources with GIS and Matlab tools to reproduce the correct wave dynamics during the inundation computation. Water depths and surface elevations are employed to estimate the wave height, wave arrival time, current velocities and inundation. Grids are based on SRTM land topography (http://www2.jpl.nasa.gov/srtm) and GEBCO bathymetry (http://www.gebco.net) data and interpretation of photos from Google earth regarding the typical offsets from buildings. Grids A and B are based on GEBCO (30 arc-second resolution) while C grid merged from STRM (90 m), local bathy (2 m), and GEBCO (900m). Finally grids are resembled to the desired resolution. The resolutions in meters are approximately 40 m (C), 150 m (B), and 600 m (A), but given in longitude latitude. Correction of SRTM data is done by subtracting a raster with 4 m elevation values in each cell from the original SRTM surface raster. It is a crude interpretation of pictures from Google earth. We estimated the height of buildings 4 to 5 m, but this may be erroneous. SRTM is a digital surface model (DSM) including forest and a settlement in the height information, therefore this subtraction was done. The values which became negative due to this were set to 2 m afterwards.
After visual interpretation of topography, the local bathymetry was transferred from UTM to Geographical Coordinates (longitude-latitude) and the prefix of the Z values changed to negative values. The shoreline is digitized, by assigning Z values = 0, to have a clear border between land and water. Then we merged all point data sets GEBCO, local bathymetry, shore line and corrected SRTM to one point data set by the method of TIN (Triangulated Irregular Network) interpolation. Figure 3 defines the TIN interpolation.

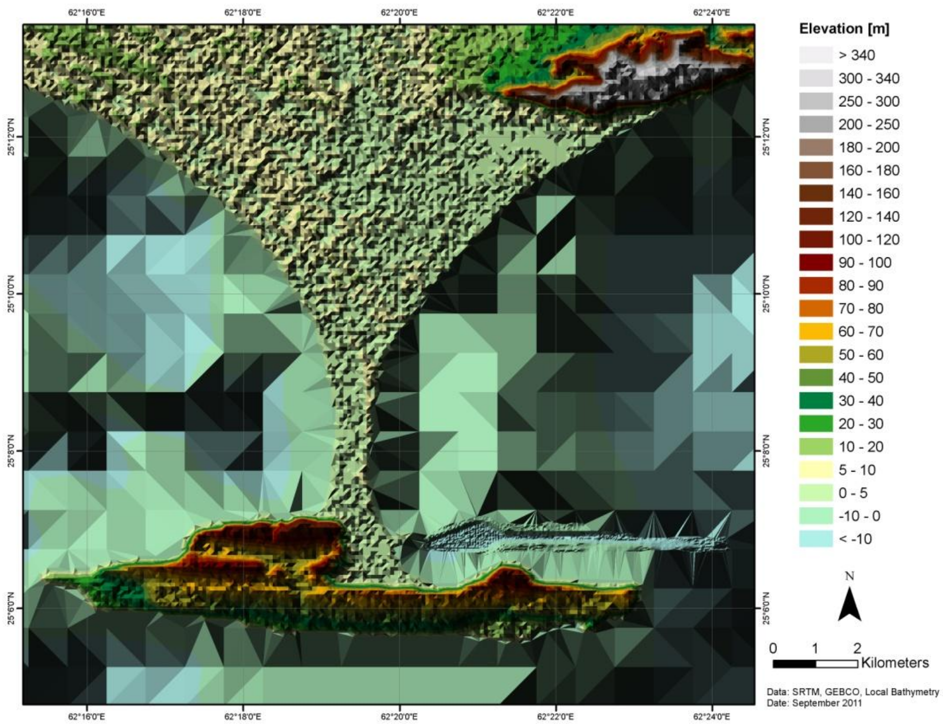

Figure 3 Final TIN for the elevation data around Gawadar

TIN data set is then converted to a regular raster with 40 m resolution for C-grid Figure 4 defines the forecast point where A and B grids are based on GEBCO only.

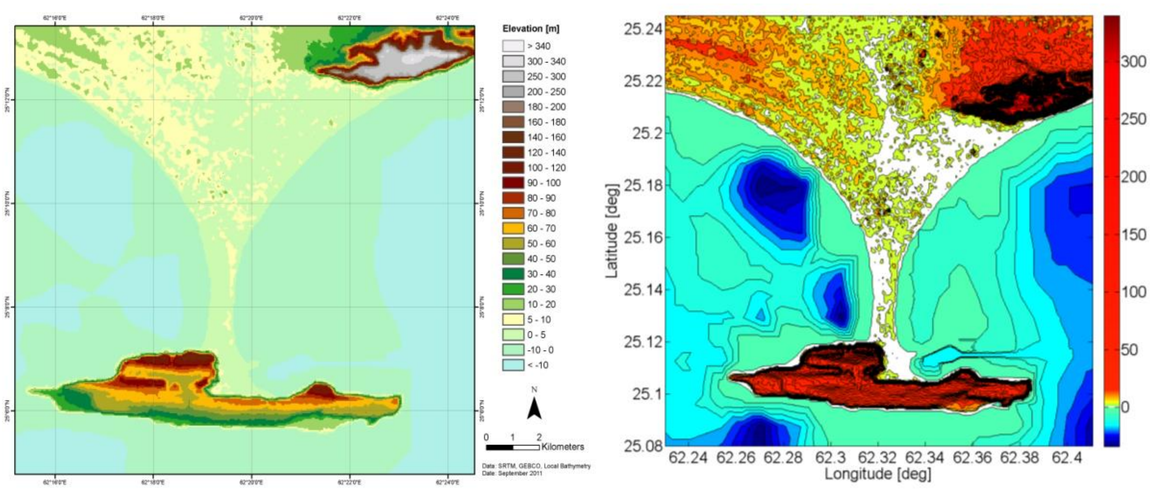

Figure 4 Final topography and bathymetry converted from TIN to Raster (a) and bathymetry contours plot around Gwadar (b)

Three nested rectangular grids (A, B and C) that shrivel down from a large extent to a finer C grid are shown graphically in Figure 5, 6 and 7.

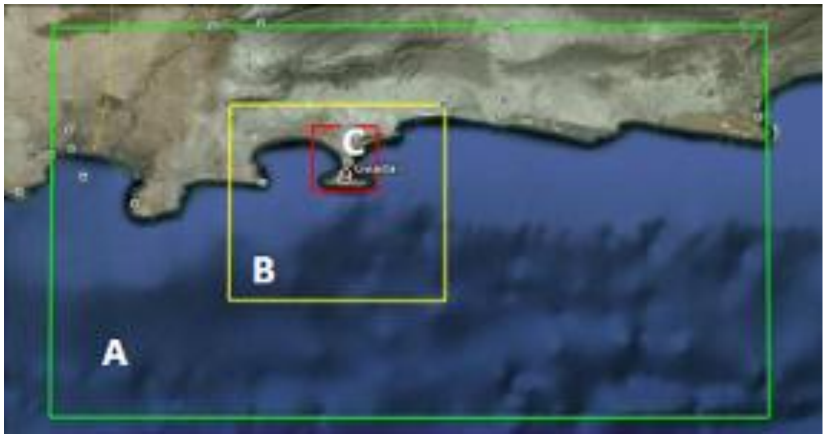

Figure 5 Extents of grids A, B and C at Gwadar

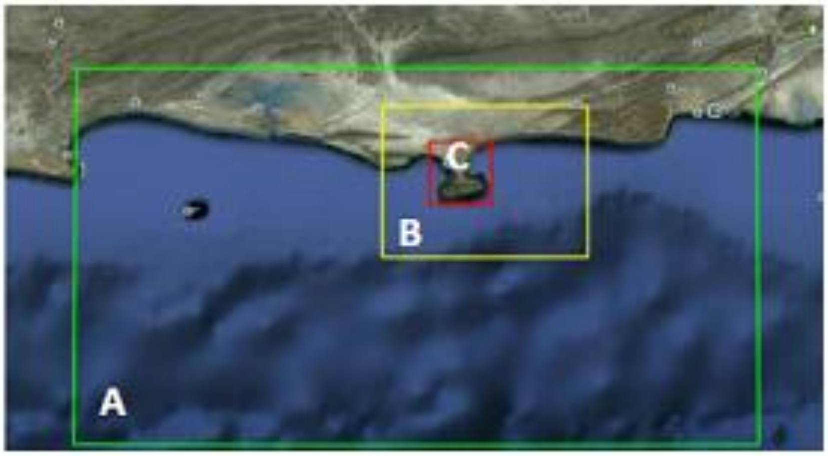

Figure 6 Extents of grids A, B and C at Ormara

Figure 7 Extents of grids A, B and C at Pasni

Detail parameters for forecast model grids, including extents are summarized in Tables 1, 2 and 3.

Table 1 Grids A, B and C resolution for Gwadar

Grids	Extent	Resolution (m)	Cell Size Nx × Ny	Max. Depth (m)	Max. Elev. (m)	CFL (s)
A	24.5000-25.4960 °N 61.5000-63.4980 °E	600	334×167	-2390.5	774.9	3.99
B	24.8000-25.2995 °N 62.0000-62.6000 °E	150	401×334	-1349.4	269.4	1.32
C	25.0799-25.2451 °N 62.2301-62.4108 °E	40	503×460	-33.8	343.7	1.99

Table 2 Grids A, B and C resolution for Ormara

Grids	Extent	Resolution (m)	Cell Size Nx × Ny	Max. Depth (m)	Max. Elev. (m)	CFL (s)
A	24.5000-25.4960 °N 61.5000-63.4980 °E	600	334×167	-2390.5	774.9	3.99
B	24.8000-25.2995 °N 62.0000-62.6000 °E	150	401×334	-1349.4	269.4	1.32
C	25.0799-25.2451 °N 62.2301-62.4108 °E	40	503×460	-33.8	343.7	1.99

Table 3 Grids A, B and C resolution for Pasni

Grids	Extent	Resolution (m)	Cell Size Nx × Ny	Max. Depth (m)	Max. Elev. (m)	CFL (s)
A	24.5000-25.4960 °N 62.5000-64.4980°E	600	334×167	-2549.5	775.3	3.85
B	25.000-25.3990°N 63.2000-63.8000°E	150	401×267	-84.5	118.0	5.26
C	25.1708-25.3379 °N 63.3709-63.5541°E	40	510×465	-14.0	115.8	3.10

Where minimum offshore depth is taken as 0.2m; water depth for dry land as 0.1m and friction coefficient ($n^{2)}$ is equal to 0.0009m for all the three grids.

3. Numerical Tsunami Simulation

Numerical modeling of tsunami is an important tool of tsunami studies in scientific research. Tsunami modeling is necessary for better preparedness and mitigation against tsunami disaster.

3.1 Method of Splitting Tsunami (MOST)

Numerical model used to compute the tsunami inundation in this study is Method of Splitting Tsunami MOST (Titov and Synolakis. 1998). The accuracy and efficiency of this model tested and validated (see e.g. Titov and Gonzalez, 1997, Titov and Synolakis, 1998).

3.2 Governing Equations

Nonlinear shallow water wave equations are solved to compute inundation at the coast

$$h_t + (uh)_x + (vh)_y = 0$$

$$u_t + uu_x + vu_y + gh_x = gd_x,$$

$$v_t + uv_x + vv_y + gh_y = gd_y.$$

where $h = \Delta(x,y,t) + d(x,y,t)$, where $\Delta(x,y,t)$ is the surface elevation, and $z = -d(x,y,t)$ is the location of the bottom with respect to the undisturbed water surface, while $u(x,y,t)$, $v(x,y,t)$ are the depth-averaged velocities in the longitudinal (x) and latitudinal (y) directions respectively; g is the gravitational acceleration($g=9.8 m/s^2$).

3.3 Input Parameters

The input parameters used to run the model are depicted in Table 4:

Table 4 Parameters to run Model

Model Input Parameters	Values
Minimum amplitude of input offshore wave (m)	0.005
Minimum depth for offshore (m)	0.2
Dry land depth inundation (m)	0.1
Friction coefficient (n**2)	0.0009
Max eta before blow-up (m)	300
Time step (sec)	1.2500
Total number of steps in run	11500
Time steps between A-Grid computations	3
Time steps between A-Grid computations	1
Time steps between output steps	24
Save output every n-th grid point	1

3.4 Courant Friedrics Lewy Condition (CFL)

Numerical stability of the model is ensured by considering the CFL (Courant Friedrics Lewy) condition given by the following formula:

$$\Delta t \leq \frac{\Delta x}{\sqrt{2gh_{\max}}}$$

Here, Δx is spatial grid size, Δt is temporal grid size, g is acceleration due to gravity and *hmax* is the greatest sea depth in the calculated area. If the temporal grid size was set at more than the CFL condition, the numerical simulations would result with instability.

3.5 Scaling Law

Scaling law theory is used to determine the fault parameters such as length, width and slip amount (Coppersmith & Wells 1994). This theory is useful to calculate the parameter of earthquake events, which is controlled by moment magnitude. The equations of scaling law theory are expressed as follows:

$$\log L = 0.5M_W - 1.9$$

$$W = \frac{L}{2}$$

$$\log U = 0.5M_W - 1.4$$

Here, L is length (km), W is width (km), U is slip amount (cm) and Mw is moment magnitude.

Fault plane parameters used to estimate the vertical deformation of the sea floor are described and illustrated in Table-5 and Figure 8 respectively. The dislocation of the ocean bottom can be estimated from Wells and Coppersmith fault plane parameters (Wells and Coppersmith 1994). Shallow earthquakes are more efficient in generating tsunamis than deep earthquakes. Usually, only the vertical component of the ocean bottom is considered for tsunami generation.

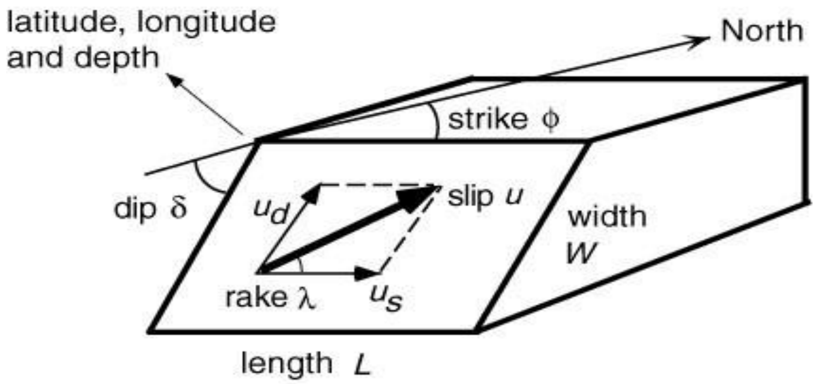

Figure 8 Fault plane parameters (Satake, 2008)

To compute the surface deformation, the fault parameters such as fault location, geometry (strike, dip and rake), size (length L and width W) and average slip U need to be defined first. The seismic moment *Mo* is given as

$$M = \mu US = \mu ULW$$

where *S* is the fault area and μ is rigidity. Thus, the moment magnitude is defined as;

$$M_W = \frac{\log M_0 - 9.1}{1.5}$$

The scenarios are constructed based on superposition of available sources in MOST, which is also the simulation tool applied in the current study.

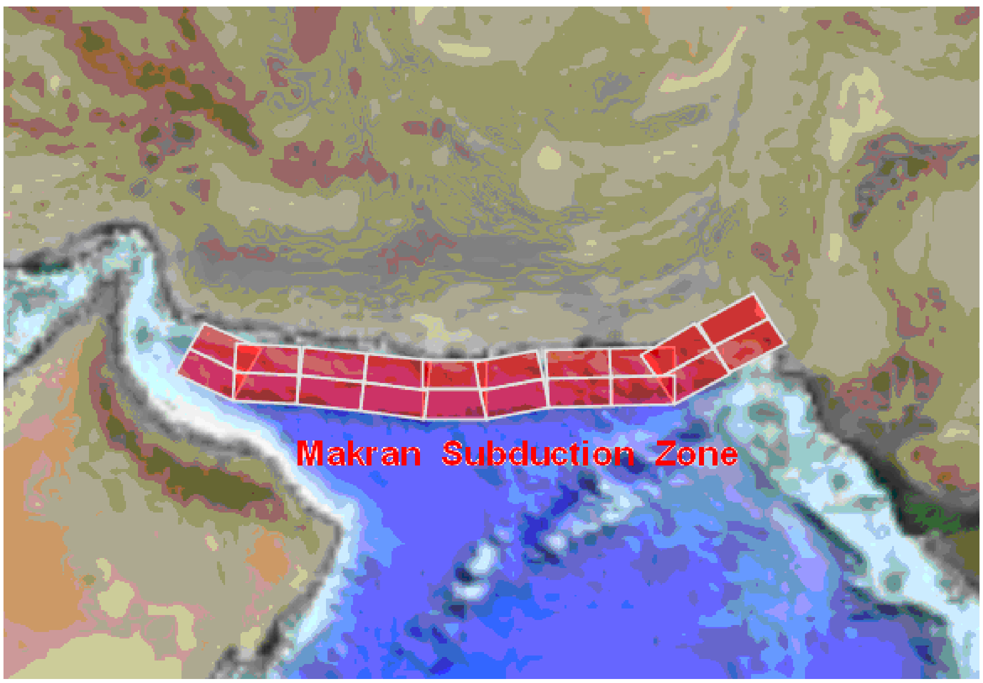

Figure 9 Earthquake source along Makran Subduction Zone

The rectangular boxes in Figure 9 represent the earthquake sources along Makran Subduction zone. The specific information about these sources summarized in Table 5. These parameters are adopted from Coppersmith and Wells model.

Table 5 Fault Plane Parameters

Fault Plane (Source)	*Lat (°N)*	*Long (° E)*	*Strike*	*Dip*	*Rake*	*Depth (km)*	*Length (km)*	*Width (km)*
mksza1	65.8163	25.8503	239.612°	3.0°	90°	7.62	100	50
mkszb1	66.0688	25.4637	239.612°	3.0°	90°	5.00	100	50
mksza2	64.9317	25.3606	237.752°	3.0°	90°	7.62	100	50
mkszb2	65.1970	24.9817	237.752°	3.0°	90°	5.00	100	50
mksza3	64.5214	25.2436	268.831°	3.0°	90°	7.62	100	50
mkszb3	64.5315	24.7952	268.831°	3.0°	90°	5.0	100	50

mksza4	63.5221	25.2159	267.657°	3.0°	90°	7.62	100	50
mkszb4	63.5424	24.7677	267.657°	3.0°	90°	5.00	100	50
mksza5	62.4110	25.1007	259.36°	3.0°	90°	7.62	100	50
mkszb5	62.5027	24.6599	259.36°	3.0°	90°	5.00	100	50
mksza6	61.6246	25.0339	270.00°	3.0°	90°	7.62	100	50
mkszb6	61.6246	24.5854	270.00°	3.0°	90°	5.00	100	50
mksza7	60.7661	25.0821	276.99°	3.0°	90°	7.62	100	50
mkszb7	60.7057	24.6369	276.99°	3.0°	90°	5.00	100	50
mksza8	59.7748	25.1917	276.858°	3.0°	90°	7.62	100	50
mkszb8	59.7155	24.7465	276.858°	3.0°	90°	5.00	100	50

In near shore sense, ground deformation, the maximum sea water displacement and the dip angle play important role in assessing the coastal effect (Taide et al., 1996). The applied MOST sources are interpreted with a very shallow dip which most likely to underestimate the height of the initial elevation, and as a consequence, the run-up.

4 Results and Discussions of Numerical Modeling

4.1 Case Scenarios

A range of earthquake source scenarios including moment magnitudes 7.7, 8.1, 8.5, and a mega thrust of 9.0 were simulated. As expected, simulation results (summarized in Table 6-8 and plotted in set of Figures 10-21) showed the most destructive tsunamis to the cities of Gwadar, Pasni and Ormara with the scenarios for magnitude Mw 9.0 and 8.5. The first tsunami wave approaches the coast within 12 –20 minutes at Gwadar, 17-20 minutes at Ormara and 25-31 minutes at Pasni after the origin time of dislocation. The narrow land strips of Gwadar and Ormara hammer shaped peninsulas are completely inundated in Mw 9.0 scenario with a maximum water level of 7.5m above normal high tide, however tides are not taken into account for our analysis.

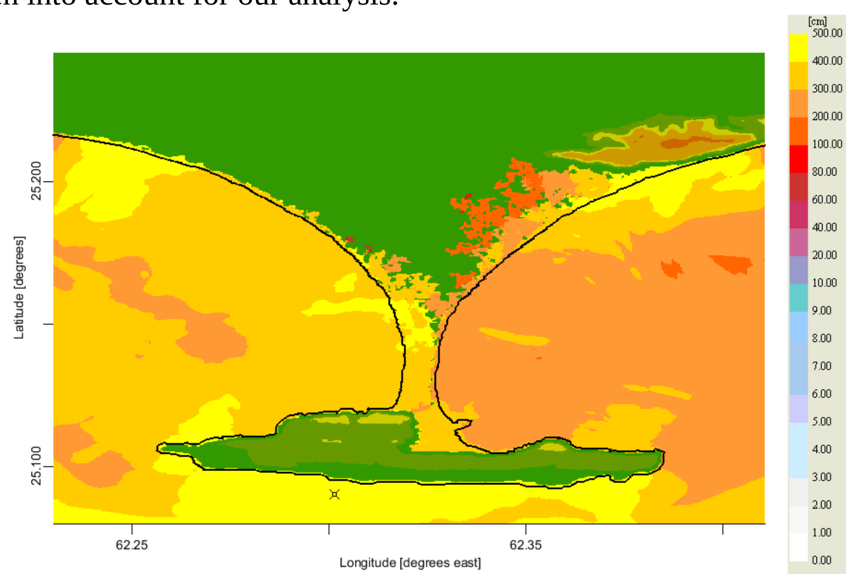

Figure 10 Maximum inundation at Gwadar for Mw 9.0

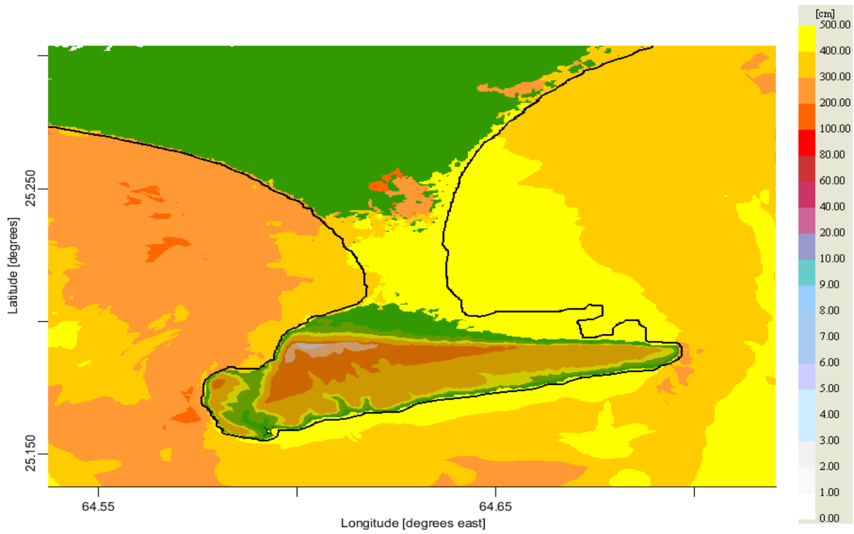

Figure 11 Maximum inundation at Ormara for Mw 9.0

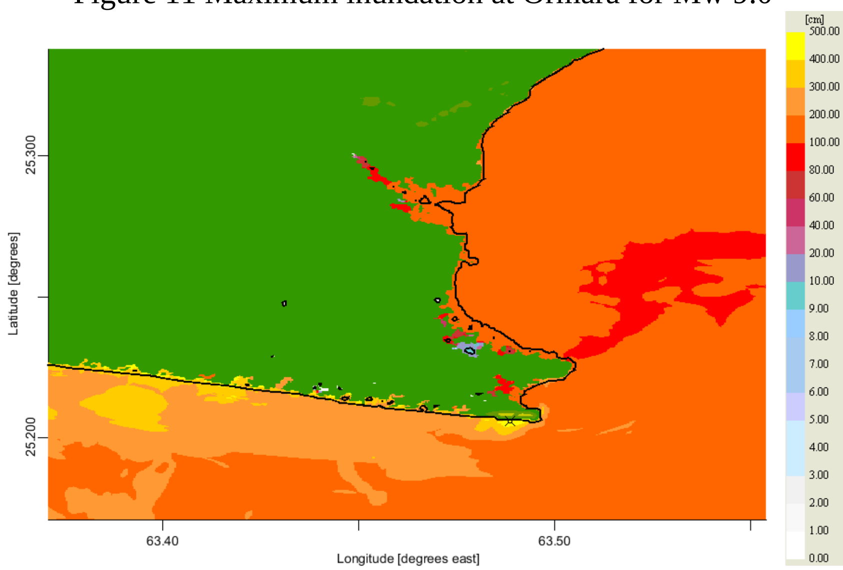

Figure 12 Maximum inundation at Pasni for Mw 9.0

The waves refracted from east and west over top the narrow strips of both cities. Pasni is inundated up to 1.2km at some locations with a maximum water level of 5.4m. A river flowing on the northern sides of Pasni gets inundated up to 3km which could be a potential threat for the city. The river may overflow from its banks due to this heavy inundation, leading to complete flooding with strong currents. Subsequent oscillations are still present during the 4 hours simulation.

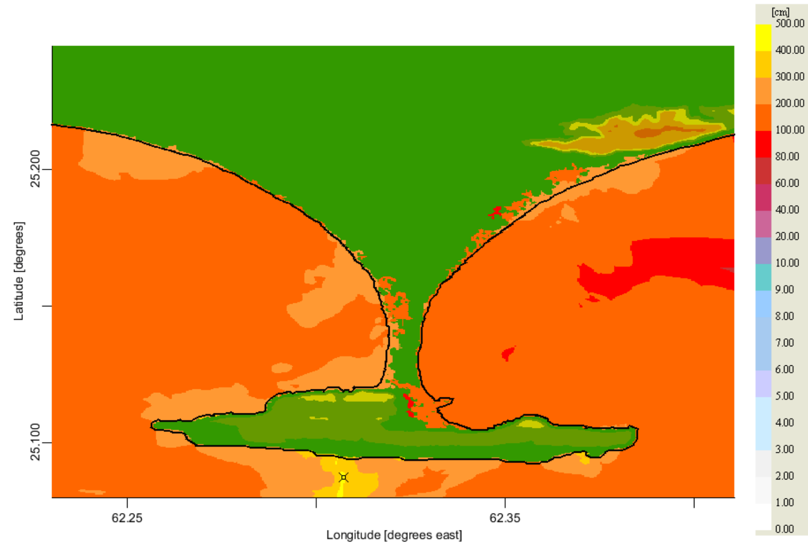

Figure 13 Maximum inundation at Gwadar for Mw 8.5

Again maximum area of Gwadar and Ormara is inundated in Mw 8.5 scenario with a maximum water level of about 4m, where as harbor area is completely inundated. Some areas of Pasni are also inundated with water level of about 3.7m and at the same time the river inundated1.3km.

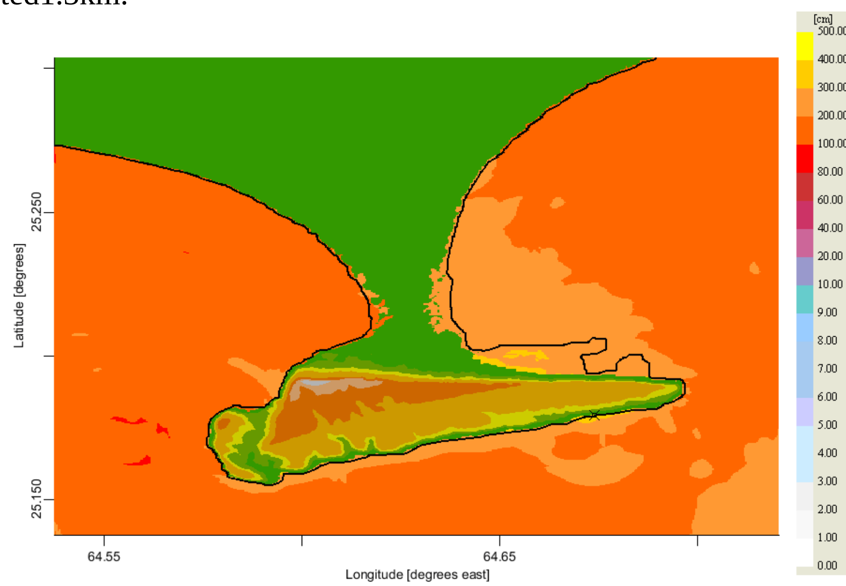

Figure 14 Maximum inundation at Ormara for Mw 8.5

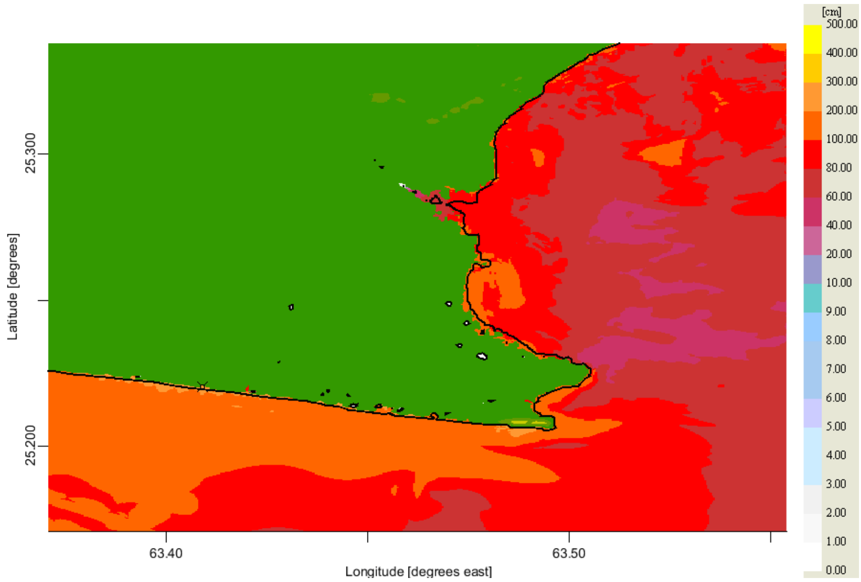

Figure 15 Maximum inundation at Pasni for Mw 8.5

In scenario with Mw 8.1, maximum run up height is approximately 1-2m, with a slight inundation where as the computed maximum wave height in scenario with Mw 7.7 is nearly 0.1-0.4m and none of the area is inundated

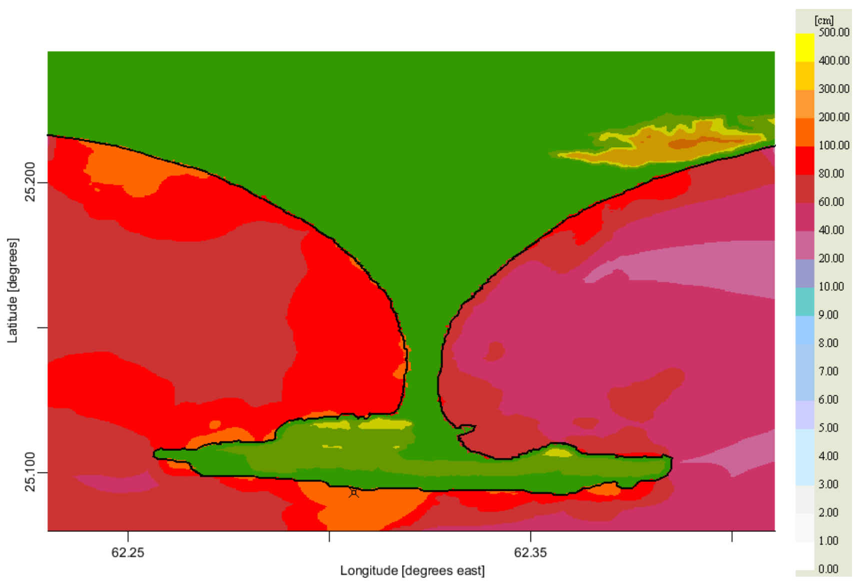

Figure 16 Maximum inundation at Gwadar for Mw 8.1

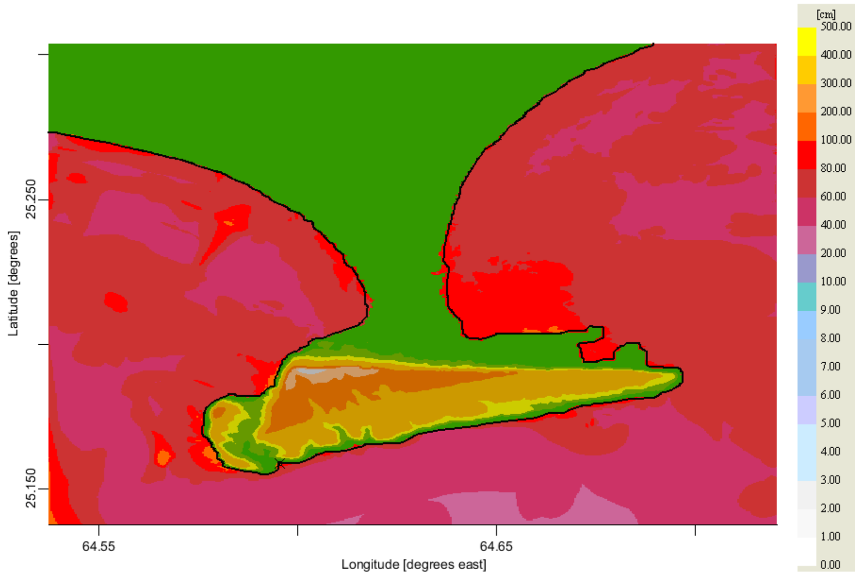

Figure 17 Maximum inundation at Ormara for Mw 8.1

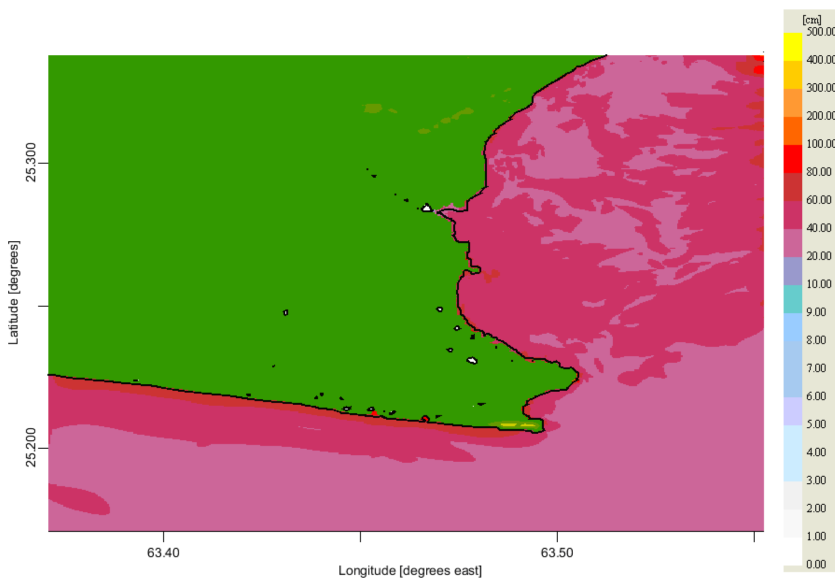

Figure 18 Maximum inundation at Pasni for Mw 8.1

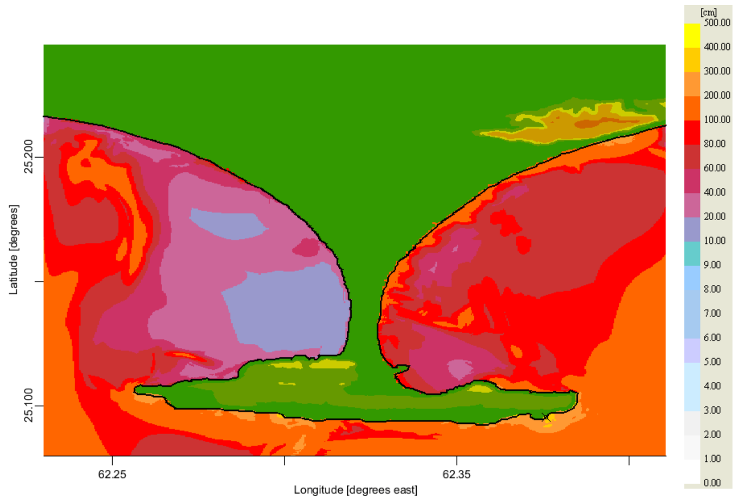

Figure 19 Maximum inundation at Gwadar for Mw 7.7

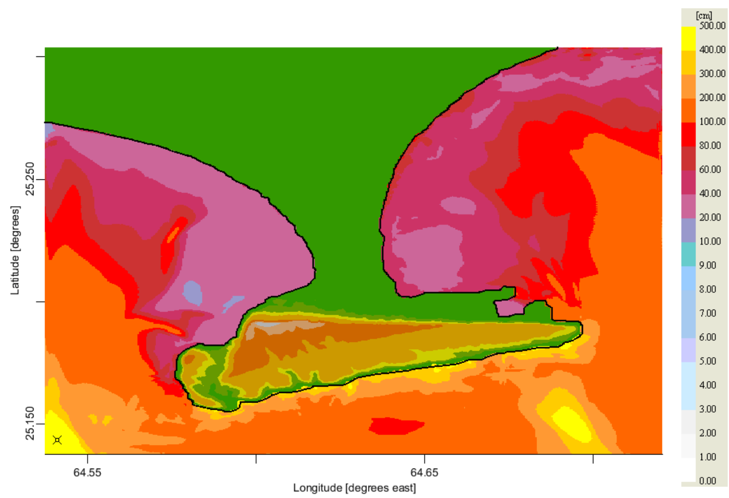

Figure 20 Maximum inundation at Ormara for Mw 7.7

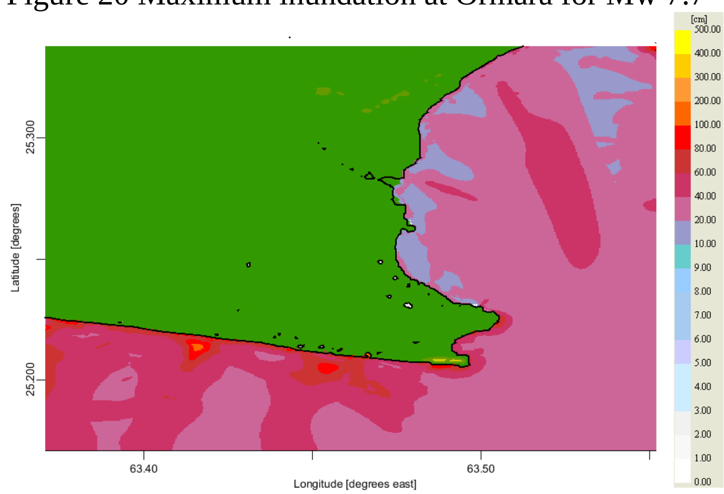

Figure 21 Maximum inundation at Pasni for Mw 7.7

The computed maximum wave amplitude and current velocities (flow velocities) are found to be in the range of 7-11 m/s and 4-6 m/s in the case scenario of Mw9.0 and 8.5 respectively shown in Figure 22, 23 and 24.

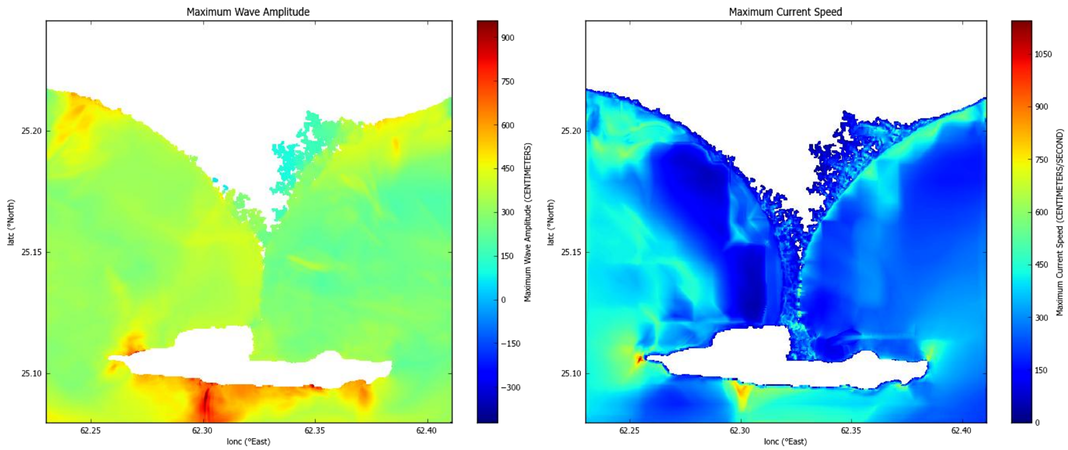

Figure 22 Maximum wave amplitude (a) and current speed (b) at Gwadar Mw 9.0

Table 6 Arrival Time and height of the first maximum and the highest maximum at Gwadar

Dislocation Model	First Maximum	Highest Maximum
Mw 9.0	1.4m @ 12 minutes	7.5m @ 18 minutes
Mw 8.5	01m @ 20 minutes	4.2m @ 22 minutes
Mw 8.1	0.5m @ 21 minutes	1.7m @ 26 minutes
Mw 7.7	0.09m @ 25 minutes	0.5m @ 37 minutes

These velocities could be attributed to produce very high momentum, causing everything to sweep up. The tsunami waves of less run-up values may not be under-estimated because of their very different nature as compared to short period oscillations like wind waves because of their high momentum while over-toping small, flat strips like Ormara and Gwadar.

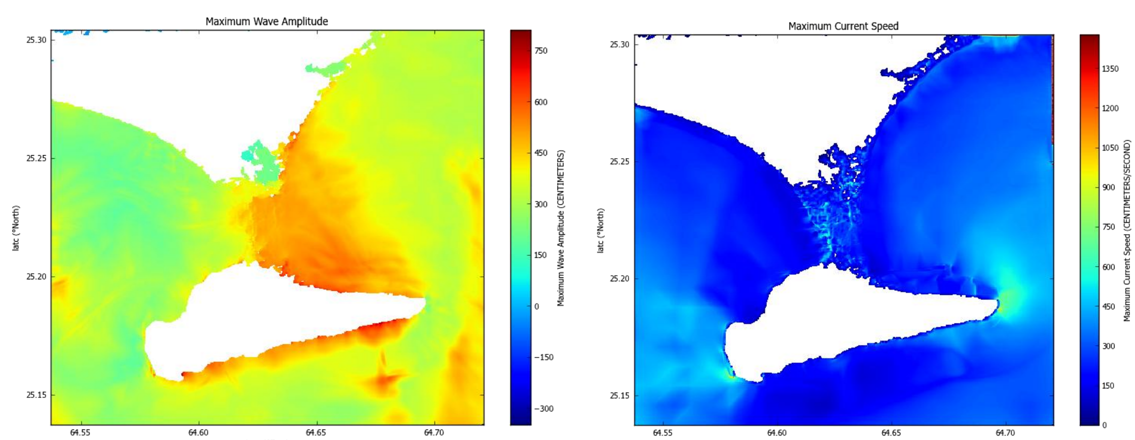

Figure 23 Maximum wave amplitude (left) and current speed (right) at Ormara Mw 9.0

Table 7 Arrival Time and height of the First maximum and the highest maximum at Ormara

Dislocation Model	First Maximum	Highest Maximum
Mw 9.0	1m @ 17 minutes	6m @ 23minutes
Mw 8.5	0.8m @ 20 minutes	3.9m @ 27 minutes
Mw 8.1	0.3m @ 21 minutes	1.2m @ 32 minutes
Mw 7.7	0.09m @ 25 minutes	0.4m @ 44 minutes

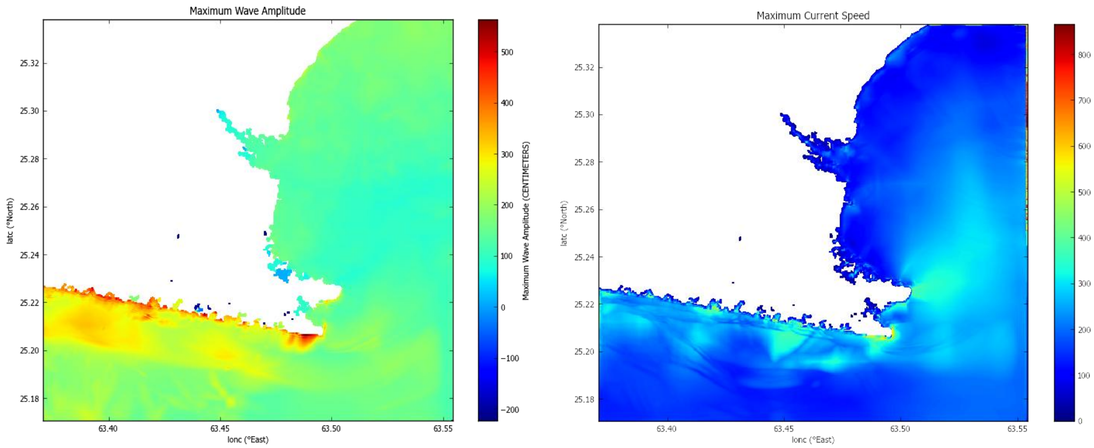

Figure 24 Maximum wave amplitude (a) and current speed (b) at Pasni Mw 9.0

Table 8 Arrival Time and height of the first maximum and the highest maximum at Pasni

Dislocation Model	First Maximum	Highest Maximum
Mw 9.0	0.4m @ 21 minutes	5.4m @ 38minutes
Mw 8.5	0.1m @ 31 minutes	3.7m @ 42 minutes
Mw 8.1	0.06m @ 35 minutes	1m @ 46 minutes
Mw 7.7	0.02m @ 40 minutes	0.1m @ 51minutes

4.2 Time Histories

The time history graphs illustrated below in Figure 25-30, for some random point locations. The origin of the time axis is defined as the origin time of dislocation. Vertical axis indicates water level in meters relative to mean sea level at a reference point. In each case the start of tsunami indicates the uplift of the shore.

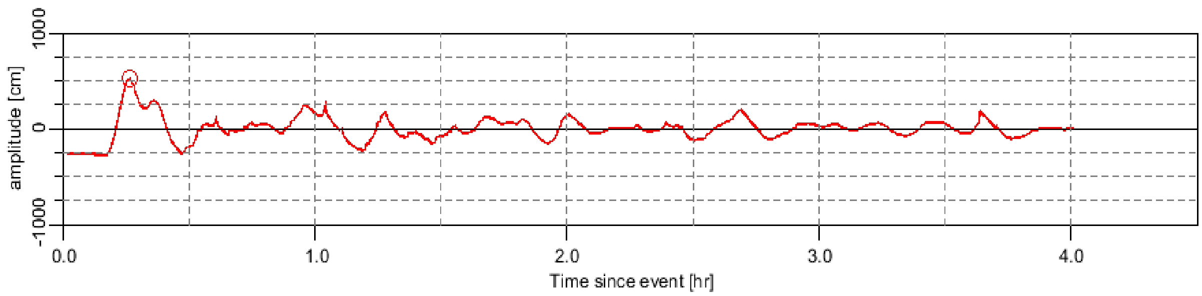

Figure 25 Time histories at Gawadar (Mw 9.0), shows first maximum wave (small circle)

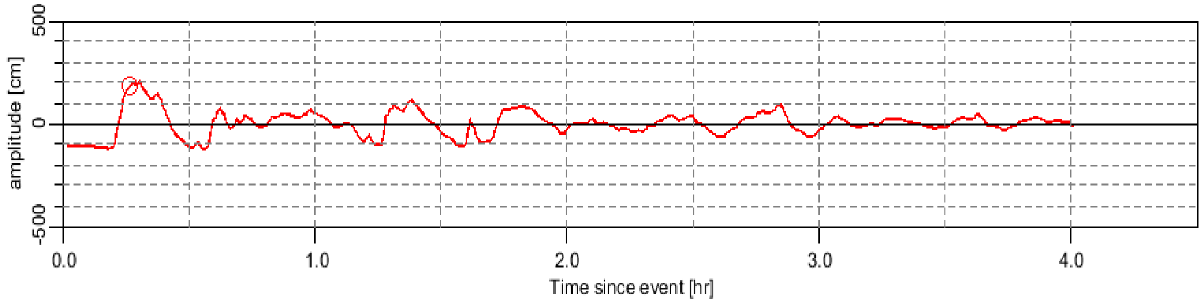

Figure 26 Time histories at Gwadar (Mw 8.5), shows first maximum wave (small circle)

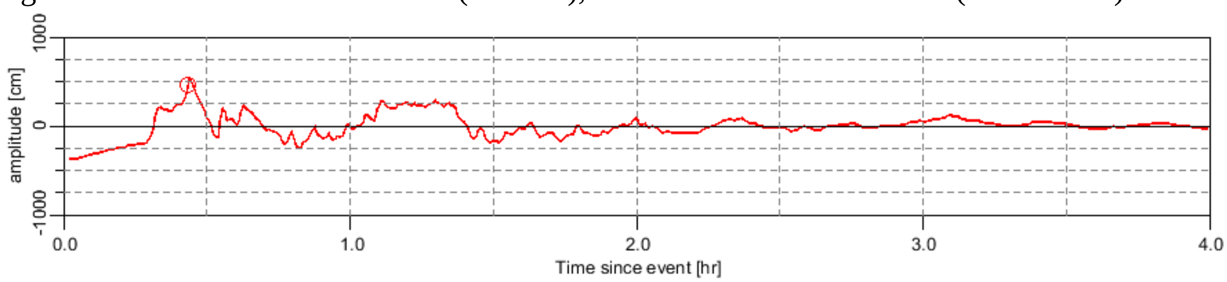

Figure 27 Time histories at Ormara (Mw 9.0), shows first maximum wave (small circle)

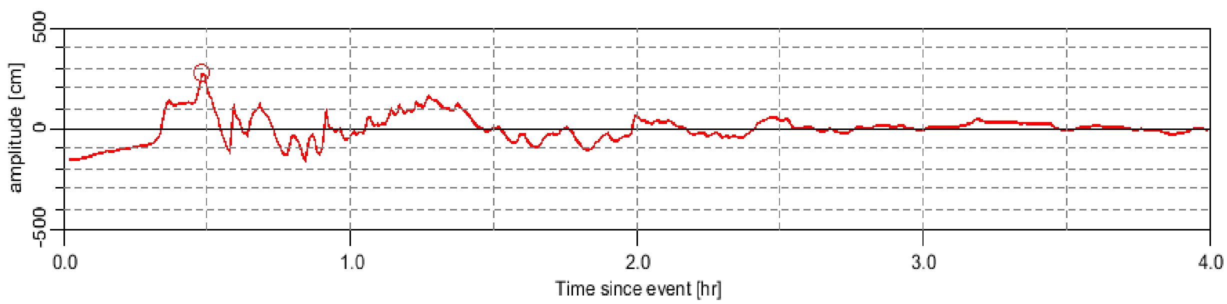

Figure 28 Time histories at Ormara (Mw 8.5), shows first maximum wave (small circle)

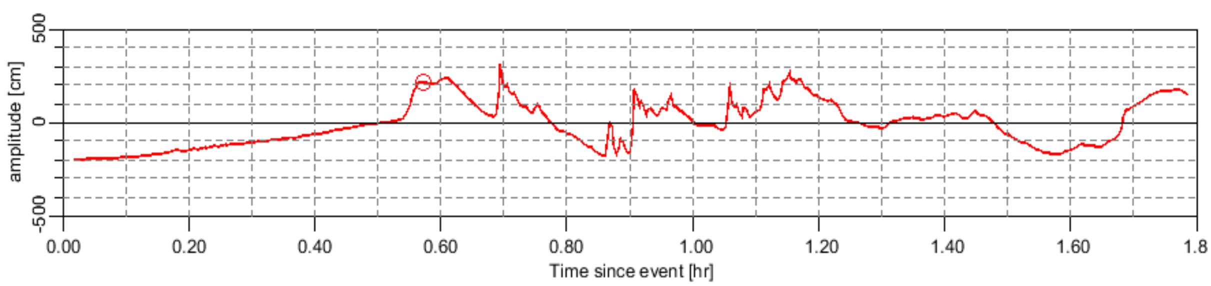

Figure 29 Time histories at Pasni (Mw 9.0), shows first maximum wave (small circle)

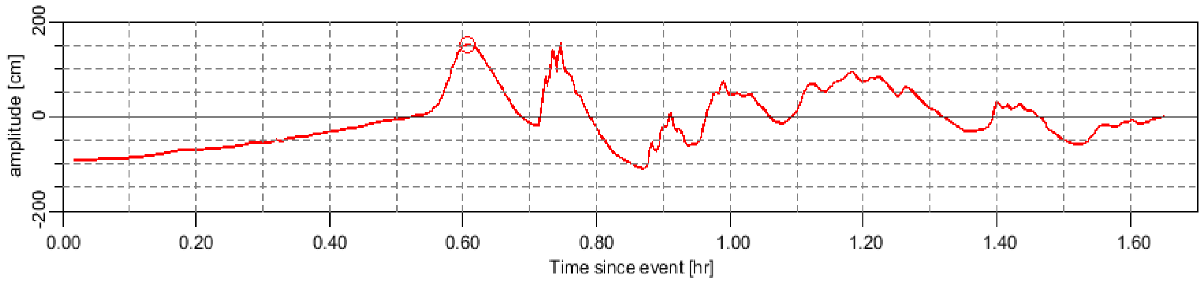

Figure 30 Time histories at Pasni (Mw 9.0), shows first maximum wave (small circle)

5. Discussions and Conclusions

We evaluate the earthquake tsunami hazard along the Makran Subduction zone for three coastal cities Gwadar, Ormara and Pasni. We use numerical model MOST to estimate inundation due to tsunami scenarios It can be assumed from the simulation results that Makran Subduction Zone can expect a tsunami, capable of inflicting catastrophic damage to life and infrastructures at the coast. Based on the results of our modeling we find that the narrow, nearly flat, strips of Gwadar and Ormara, are inundated almost to their full extent, with a water level of about 5-7m in case scenarios with Mw 9.0 and significant inundation with water level of 4m in case scenario with Mw 8.5. The next parameter which is required to be investigated is overland flow velocities. High flow velocities of tsunami waves, over-topping a narrow flat strip and propagating over it, has been identified as one of the main causes of heavy loss to life because during overland flow the kinetic energy is only reduced by dissipation (Titov et al., 1997).

The findings suggest that refined land topography and ocean bathymetry would be useful in improving the reliability of tsunami warning systems. The final results are sensitive to local bathymetric and topographic features and resolution of both bathymetric and topographic data. The computations made by MOST model reveal that the wave height may reach up to 7.5 m above mean sea level along the Makran coast. The huge difference between the reported and computed values may be either due to over estimates or we may have to investigate the reason behind this huge difference. Field surveys are essential to answer such type of uncertainties.

The 1945 Makran tsunami have some similarities with Papua-new Guinea (PNG) 1998, tsunami. A number of authors have stated, though no scientific prove is presented that 1945 Makran Tsunami was two episodic. Similarly PNG 1998, tsunami also proceeded with two episodes. The tsunami waves of 10m height arrived 10 minutes after the earthquake and that of 15m after that. Suggesting the later may have been due to landslide (Okal et al. 2008).The strong nature of disaster in near field by PNG 1998 tsunami along a short segment of the Sandaun (23 km) coast (Okal et al. 2004) is similar to 1945 Makran tsunami, in which disaster was mostly concentrated in Pasni and Ormara. This correlation strongly supports the idea that the later episode was probably due to underwater land slide triggered by the earthquake. This is just a crude approach and hypothesis requires intensive scientific exploration and field surveys for its validation.

6. Tsunami Hazard Mitigation Perspectives

The city of Gwadar and Ormara (75000 inhabitants) are located mostly along the narrow strips of hammer shaped peninsulas, 3 – 10 m elevation from mean sea level and extend northward up to 50 m high. The tsunami inundation map for Gwadar and Ormara should take the tidal level into account at the origin time of dislocation. As estimated in our study the run-up height may easily cross the highest tide level. It is expected for a small tsunami arriving at the highest tide to cause heavy inundation damage therefore, under-estimating may cause considerable tsunami risk. Similar situation can occur at Pasni and hazard map for this city should focus on the river flooding due to inundation. Therefore identification of evacuation routes and evacuation sites should be given due importance while planning tsunami hazard mitigation.

7. Limitations

- The accuracy of the modeling results is subject to limitations in the accuracy of suitable topography and bathymetric data. Although an attempt has been made to identify a credible upper bound to inundation and maximum wave heights at the selected locations, it remains possible that actual inundation could be greater in a major tsunami event. Reliable bathymetric data is available from various sources but topography data requires to be updated by measurements with differential GPS.

- The applied MOST sources are interpreted with a very shallow dip (3.0°) which most likely underestimate the height of the initial elevation, and as a consequence, the run-up. Additional simulations with increased dip angle should therefore be carried out in a later stage.

- Tsunami dynamic is strongly dependant on, how the approaching wave especially the wavelength is modified during the course of its propagation towards the shore. Longer the wavelength of incoming wave more we get the inundation. In case of Ormara and Gwadar the wave approaches the narrow peninsulas from two sides after being diffracted from the edge of frontal high lands and entering into the curvilinear shaped bays. Frequency-magnitude statistic could help for evaluation of a possible tsunami hazard.

- The source width is playing very important role in inundation at Gwadar and Ormara. More the width of the source more it gives the inundation. The computational grids also need further amendment.

8. Recommendations

- Mapping the possible tsunami hazard is a first step towards a tsunami resistance community. The overall objective of study is to insure improved tsunami hazard assessments while taking into account the location of earthquake sources, leading to setup a reliable early warning system. This system should satisfy not only the scientific community but also the system involved in risk warning and hazard mitigation.

- All the three cities of study area are found to be most vulnerable places along the coastal belt of Makran; the impact of tsunami waves can amplify when no protective structures are built up. The southern bank of the Pasni River should also be given due consideration while planning tsunami hazard, as the river can over-flow due to inundation caused by tsunami.
- The field surveys of the past events are highly desirable for comparison of observed and computed results and for further documentation.

- The study was carried out at NGI with the aim to assist the local authorities in Pakistan with development of plans for how to deal with the future tsunami hazard and risk along Makran coast in a short term, as well as in a long term perspective.

- It is essential to use high-resolution models in order to provide accuracy that is useful for the practical guidance of coastal tsunami forecasts. Since the first peak of the synthetic tsunami in Gwadar arrives at the open coast and at the harbor 12 – 20 minutes after the origin time of the dislocation. There is little time for the national tsunami early warning system to alert coastal residents that danger is imminent, therefore a local community based warning system may be helpful for immediate evacuation announcement. However, adjacent hills (koh batal) south of the narrow strip of Gwadar may offer secure evacuation place on feeling the earthquake shaking, people evacuate to higher ground. In case of local generated tsunami like the one simulated here, the best mitigation strategy is to create a tsunami aware community. As almost all inhabitant areas are found prone to inundation, some robust vertical evacuation sites may be constructed within 10 minutes of walking distance.

- Four steps are critical to create a tsunami resistant community;

  a) produce tsunami inundation/hazard maps to identify areas susceptible to tsunami flooding
  b) implement and maintain an awareness / educational programs on tsunami dangers,
  c) Develop early national warning system to alert coastal residents that danger is imminent.

d) Develop local tsunami early warning system to alert the coastal community without waiting for the warning received from national early warning system

The first and third steps have been successfully accomplished for all the three important cities located along the Makran coast of Pakistan. Evacuation routes and emergency shelter locations should be indicated in the hazard map to help the population and local authorities in the event of a future tsunami occurrence. It remains for Pakistan to develop a reliable local early warning system and implement an awareness program for tsunami prevention.

References

Ambraseys, N.N. and C. P. Melville: A History of Persian Earthquakes, Cambridge Earth Science Series. xvii, 219 pp. Cambridge, etc.: Cambridge University Press, 1982.

Donald L. Wells and Coppersmith K. J: New empirical relationships among magnitude rupture length, rupture width, rupture area, and surface displacement, Seismological Society of America, Vol. 84, No. 4, pp 1974-1002, 1994.

Emile A. Okal and Costas E. Synolakis: Far-field tsunami hazard from mega-thrust earthquakes in the Indian Ocean, Geophys. J. Int. (2008) 172**,** 995–1015

Farhoudi, Godratollah, Karig D. I: Makran of Iran and Pakistan as an active arc system. Geology, vol.5 Issue 11, p.664, 1977.

Harms J. C., Cappel H. N., Francis D. C (1982): Geological and Petroleum potential of the Makran Coast, Pakistan, Society of Petroleum Engineers, Singapore. 10423-MS.

Heidarzadeh M, Pirooz MD, Zaker NH, Mokhtari (2009): Numerical Simulation of the 28 November 1945 Makran Tsunami as a tool to assess tsunami risk in southern coasts of Iran" International Conference on Seismology and Earthquake Engineering, May 2007, Tehran.

Heidarzadeh M, Pirooz MD, Zaker NH, Yalciner AC, Mokhtari M, Esmaeily A (2008): Historical tsunami in the Makran subduction zone off the southern coasts of Iran and Pakistan and results of numerical modeling. Ocean Eng 35(8&9):774–786.

Heidarzadeh M, Pirooz MD, Zaker NH, Yalciner AC: Preliminary estimation of the tsunami hazards associated with the Makran subduction zone at the northwestern Indian Ocean Hazards (2009) 48:229-243.

Imamura, F., 1995: Tsunami Numerical Simulation with the Staggered Leap-Frog Scheme, manuscript for TUNAMI code, School of Civil Engineering, Asian Inst. of Tech., 1-45.

Jaiswal RK, Singh AP, Rastogi BK: Simulation of the Arabian Sea Tsunami Propagation generated due to 1945 Makran Earthquake and its effects on western parts of Gujarat (India) Nat Hazards (2009) 48:245-258.

Mokhtari M, Fard IA, Hessami K: Structural elements of the Makran region, Oman Sea and their potential relevance to tsunamigenisis, Nat Hazards (2008) 47:185–199.

Musson R. M. W: Subduction in the Western Makran: The historian's Contribution, British Geological Survey.

Okal EA, Costas E, Synolakis: Source discriminates for near field Tsunami, Geophys. T. Int. (2004).

Page, W., 1979. Evidence for the recurrence of large-magnitude earthquakes along the Makran Coast of Iran and Pakistan, Tectonophysics, 52(1-4), 533-547.

Pendse C. G. (1946): The Mekran Earthquake of the 28th Nov.1945. Indian Meteorological Department Scientific notes Vol. X, No.125.

Sirtajuddin. A. (1969): tertiary Geology of part of south Makran, Baluchistan, west Pakistan, AAPG Bulletin, Vol. 53, issue No. 7 Pp. 1480-1499.

Titov V. V. and Gonzalez F. I. (1997): Implementation and testing of the Method of Splitting Tsunami (MOST) Model, NOAA Technical Memorandum ERL PMEL-112.

Titov V. V. and Synolakis C. A. (1998): Numerical Modeling of Tidal Wave Run up. Journal of Waterway, Port, Coastal, and Ocean Engineering 1998/157.

Titov V. V., Rabinovich A. B., Mofjeld H. O, Thomson R. E.,González1 F. I.(2005):Global Reach of the 26 December 2004 Sumatra Tsunami". Science, 309 (5743), 2045-2048.

Website 1: http://www.gebco.net/

Website 2: http://www2.jpl.nasa.gov/srtm/

Appendix: Snapshots of Tsunami Wave Propagation
Case Scenario Mw 9.0 for Gwadar

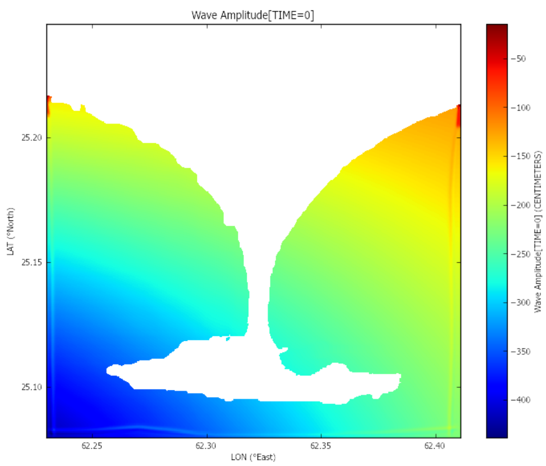

At t = 0 hour

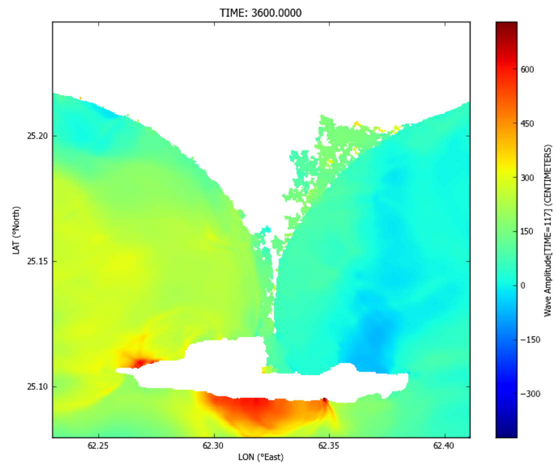

At t = 1 hour

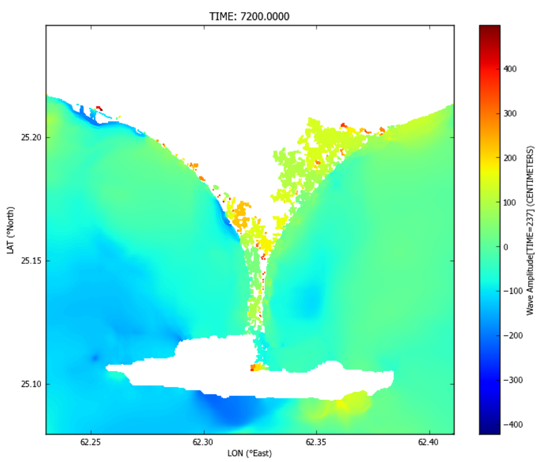

At t = 2 hour

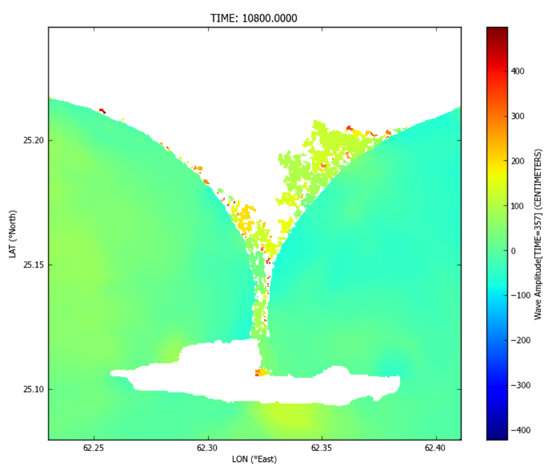

At t = 3 hour

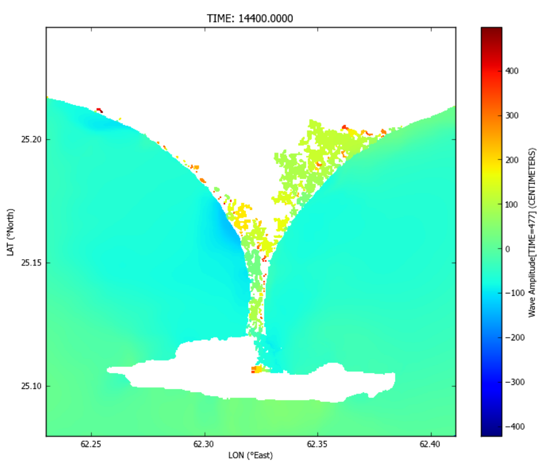

At t = 4 hour

Case Scenario Mw 9.0 for Ormara

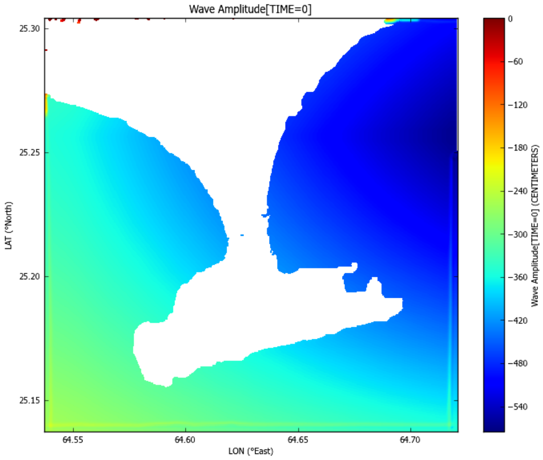

At t = 0 hour

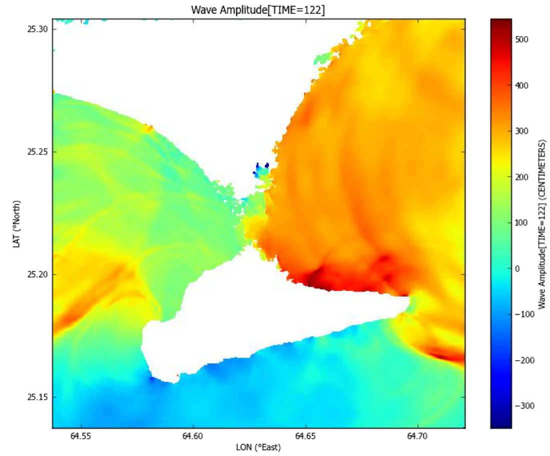

At t = 1 hour

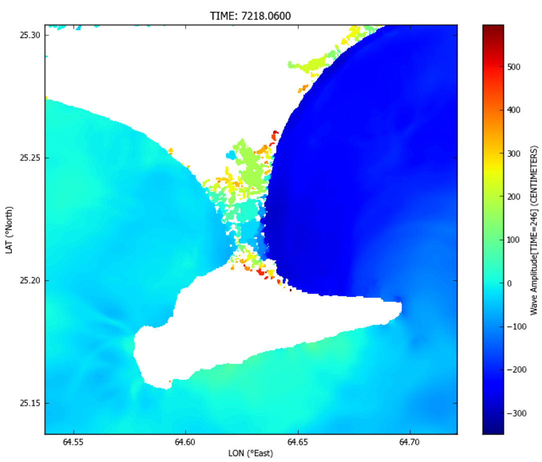

At t = 2 hour

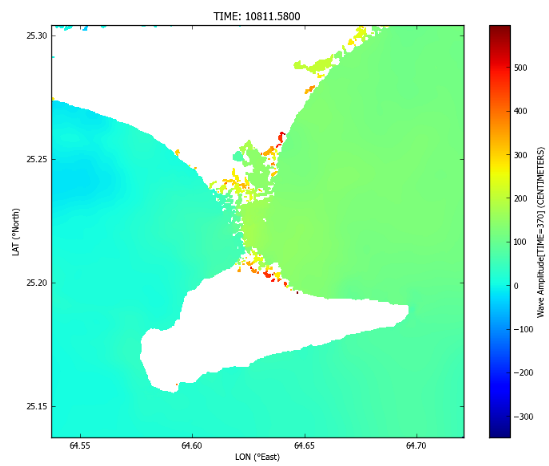

At t = 3 hour

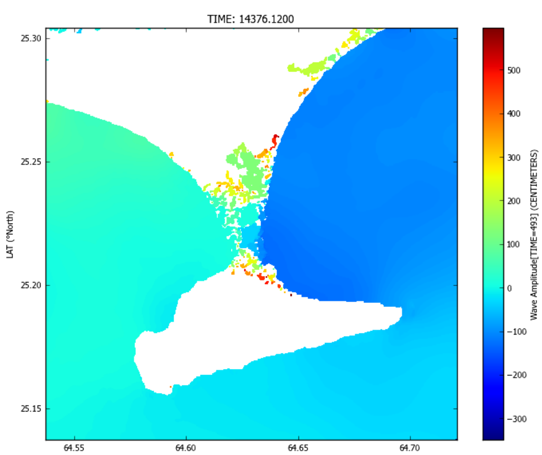

At t = 4 hour

Case Scenario Mw 9.0 for Pasni

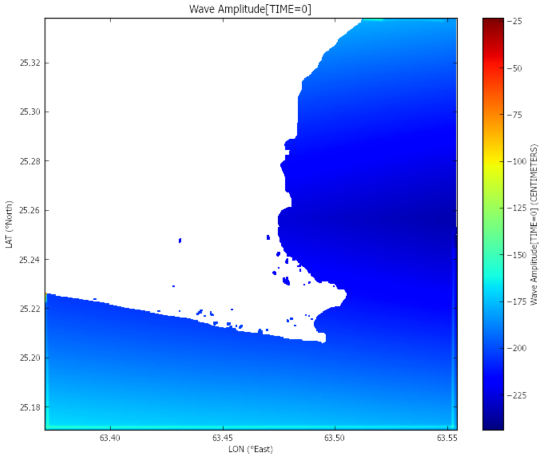

At t = 0 hour

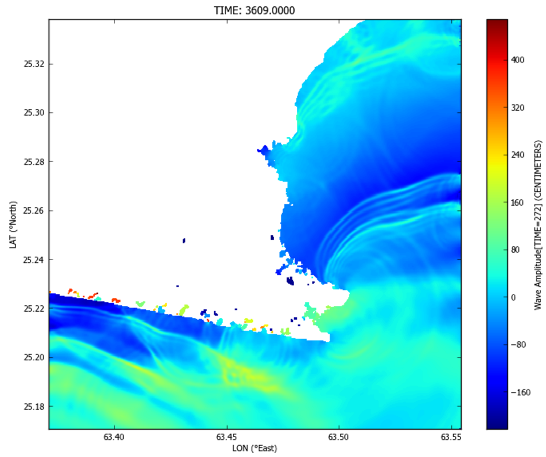

At t = 1 hour

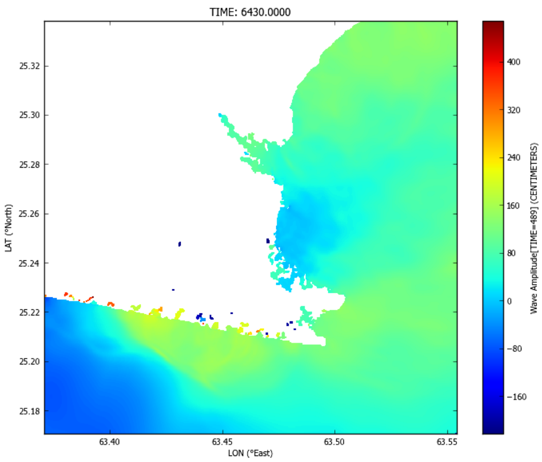

At t = 2 hour

Glossary

Arrival time: Time of the first maximum of the tsunami waves.
Accretionary wedge or Accretionary prism is formed from sediments that are accreted onto the non-subducting tectonic plate at a convergent plate boundary. Most of the material in the accretionary wedge consists of marine sediments scraped off from the down going slab of oceanic crust but in some cases includes the erosion products of volcanic island arcs formed on the overriding plate.
Bathymetry is the study of underwater depth of lake or ocean floors
Current velocity or flow velocity is a vector field which is used to mathematically describe the motion of a fluid. The length of the flow velocity vector is the flow speed. The flow velocity *u* of a fluid is a vector field

$$\mathbf{u} = \mathbf{u}(\mathbf{x}, t)$$

which gives the velocity of an element of fluid at a position $\mathbf{x}$and time$t$.
Digital Elevation Model is a digital model or 3-D representation of a terrain's surface — commonly for a planet (including Earth) — created from terrain elevation data.
Forecast Point: The location where the Tsunami Warning Centre may provide estimates of tsunami arrival time or wave height.
GIS: Geographical Information System.
GPS: Global Positioning System
Hazard is a situation that poses a level of threat to life, health, property, or environment. Most hazards are dormant or potential, with only a theoretical risk of harm; however, once a hazard becomes "active", it can create an emergency situation. A hazard does not exist when it is not happening. A hazardous situation that has come to pass is called an incident.
Horizontal inundation distance: The distance that a tsunami wave penetrates onto the shore, measured horizontally from the mean sea level position of the water's edge. Usually measured as the maximum distance for a particular segment of the coast.
Inundation: The horizontal distance inland that a tsunami penetrates, generally measured perpendicularly to the shoreline.

Inundation (Maximum): Maximum horizontal penetration of the tsunami from the shoreline. A maximum inundation is measured for each different coast or harbor affected by the tsunami.
Inundation Area: Area flooded with water by the tsunami.
Landslide is a geological phenomenon which includes a wide range of ground movement, such as rock falls, deep failure of slopes and shallow debris flows, which can occur in offshore, coastal and onshore environments.
Leading-depression wave: Initial tsunami wave is a trough, causing a drawdown of water level.
Mean Sea Level: The average height of the surface of the sea for all stages of the tide; used as a reference for elevations also called MSL.
Mega-thrust earthquakes occur at subduction zones at destructive plate boundaries (convergent boundaries), where one tectonic plate is forced under (*subducts*) another. Due to the shallow dip of the plate boundary, which causes large sections to get stuck,

these earthquakes are among the world's largest, with moment magnitudes (M_w) that can exceed 9.0.

MOST: Method of Splitting Tsunamis.

Mw: Moment Magnitude. Magnitude based on the size and characteristics of the fault rupture, and determined from long-period seismic waves. It is a better measure of earthquake size than surface wave magnitude, especially for very large earthquakes.

NGI: Norwegian Geotechnical Institute.

Period: The length of time between two successive peaks or troughs may vary due to complex interference of waves. Tsunami periods generally range from 5 to 60 minutes.

Raster: In computer graphics, raster is a **graphics** image, or **bitmap-** data structure representing a generally rectangular grid of pixels, or points of color, viewable via a monitor, paper, or other display medium.

Recession: Drawdown of sea level prior to tsunami flooding. The shoreline moves seaward, sometimes by a kilometer or more, exposing the sea bottom, rocks, and fish. The recession of the sea is a natural warning sign that a tsunami is approaching.

Risk is the potential that a chosen action or activity (including the choice of inaction) will lead to a loss (an undesirable outcome).

Run-up: Maximum height of the water onshore observed above a reference sea level. Usually measured at the horizontal inundation limit.

Sea level: The height of the sea at a given time measured relative to some datum, such as mean sea level.

Subduction Zone: A subduction zone is an area on Earth where two tectonic plates move towards one another and one slides under the other e.g. MSZ.

Thrust earthquake: An earthquake caused by slip along a gently sloping fault where the rock above the fault is pushed upwards relative to the rock below. The most common type of earthquake source of damaging tsunamis.

TIN (Triangulated Irregular Network): TIN model represents a surface as a set of contiguous, non-overlapping triangles. Within each triangle the surface is represented by a plane. The triangles are made from a set of points called mass points.

Topography is the study of Earth's surface shape and features.

Travel time: Time that it took the tsunami to travel from the source to a particular location.

Tsunami: A Japanese term derived from the characters "tsu" meaning harbor and "nami" meaning wave. Now generally accepted by the international scientific community to describe a series of traveling waves in water produced by the displacement of the sea floor associated with submarine earthquakes, volcanic eruptions, or landslides.

Tsunamigenic earthquake: Any earthquake which produces a tsunami.

Tsunamis hazard The probability that a tsunami of a particular size will strike a particular section of coast.

Tsunami Numerical Modeling: Mathematical descriptions that seek to describe the observed tsunami and its effects.

Tsunami Risk: The probability of a particular coastline being struck by a tsunami multiplied by the likely destructive effects of the tsunami and by the number of potential victims. In general terms, risk is the hazard multiplied by the exposure.

Tsunami Simulation: Numerical model of tsunami generation, propagation, and inundation.

Tsunami Source: Point or area of tsunami origin, usually the site of an earthquake, volcanic eruption, or landslide that caused large-scale rapid displacement of the water to initiate the tsunami waves.

Period of Tsunami: Amount of time that a tsunami wave takes to complete a cycle. Tsunami periods typically range from five minutes to two hours.

Water Level (Maximum): Difference between the elevation of the highest local water mark and the elevation of the sea level at the time of the tsunami. This is different from maximum run-up because the water mark is often not observed at the inundation line, but maybe halfway up the side of a building or on a tree trunk.

Universal Transverse Mercator (**UTM**) geographic coordinate system is a grid-based method of specifying locations on the surface of the Earth that is a practical application of a 2-dimensional Cartesian coordinate system.